Int. J. Devl Neuroscience 27 (2009) 669–676

Contents lists available at ScienceDirect

International Journal of Developmental Neuroscience

journal homepage: www.elsevier.com/locate/ijdevneu

# The cochlea in fetuses with neural tube defects☆

Joachim Schmutzhard [a,*], Rudolf Glueckert [a], Mario Bitsche [a], Irene Abraham [a], Christina Falkeis [b], Ilona Schwentner [a], Herbert Riechelmann [a], Bert Müller [c], Felix Beckmann [d], Consolato Sergi [d], Annelies Schrott-Fischer [a]

[a] Department of Otorhinolaryngology, Innsbruck Medical University, Anichstrasse 35, A - 6020 Innsbruck, Austria
[b] Institute of Pathology, Innsbruck Medical University, Austria
[c] Biomaterials Science Center, University of Basel, Switzerland
[d] Institute for Materials Research, GKSS-Research Center, Geesthacht, Germany

ARTICLE INFO

*Article history:*
Received 15 June 2009
Received in revised form 14 July 2009
Accepted 29 July 2009

*Keywords:*
Neural tube defects
Cochlea
Morphologic alterations
Peripherin
Beta-III-tubulin
Vimentin

ABSTRACT

In this study different malformations of the cochlea could be demonstrated. Nevertheless, we could not delineate a distinct malformation of the inner ear, that can be linked to a neural tube defect.

Neural tube defects are a frequent and heterogeneous group of malformations, ranging from the survivable spina bifida to fatal anencephaly. In multiple animal models an involvement of the vestibulocochlear system has been demonstrated. In this article human fetal temporal bones of neural tube defects were analysed in a multimodular work-up.

The morphologic study was performed with light microscopy, transmission electron microscopy and synchrotron radiation-based microcomputed tomography. Immunohistochemistry for different neuronal markers such as peripherin, beta-III-tubulin and vimentin helped to evaluate ontogenetic tissue development.

Eight fetal temporal bones with neural tube defects and five control temporal bones were included into the morphologic study. The morphologic results of the neural tube defect temporal bones showed six regularly developed cochleas and two with only a single cochlear turn. Three of the neural tube defect temporal bones were further examined with immunohistochemical analysis. No differences in the staining pattern for peripherin, beta-III-tubulin and vimentin were detected.



Neural tube defects (NTD) are a heterogeneous group of malformations, including spina bifida, encephalocele and anencephaly (Padmanabhan, 2006), with an incidence of 1 per 1000 pregnancies in the United States (Lary and Edmonds, 1996). Whereas spina bifida and encephalocele are moderately disabling forms of NTDs, compatible with survival, an anencephalic baby never achieves a conscious existence. For a deeper understanding of effects of NTD on the ontogenetic development of the inner ear studies are warranted.

The crucial embryologic period, during which the organogenesis occurs, lasts from week 3 until 8 of pregnancy (Welsch, 1992). In this gestational period the neural plate is formed and finally the closure of the neural tube takes place (Cabrera et al., 2004). The neural tube is the precursor of the central nervous and most of the peripheral nervous system (Cabrera et al., 2004). Neural tube defects result from failure of the closure of the neural tube during the embryologic development (Rintoul et al., 2002).

Till today the basic pathophysiologic mechanisms of the NTD are not fully understood. On the basis of various mutant mice strains more than 80 different mutant genes have been shown to affect the neurulation (Copp et al., 2003). Because of various animal models a major focus of the NTD studies has been set on the planar cell polarity genes (Curtin et al., 2003; Murdoch et al., 2001a; Murdoch et al., 2001b). Analysing the Looptail mouse (Lp), Crash mouse (Crsh), and the Circletail mouse (Crc) the central role of the planar cell polarity in the mechanism of neural tube closure has been shown (Doudney and Stanier, 2005). The basic role of the planar cell polarity in these mice models has been first indicated by a misorientation of the stereocilia bundles of the organ of Corti (Doudney and Stanier, 2005). These

☆ *Funding*: FWF Project B05 15958.

*Abbreviations:* AT, apical turn; BT, basal turn; C, synchotron radiation-based microcomputed tomography (Table); g, gestational age; HE, hematoxylin–eosin; I, immunohistochemisty; ID, interdental cells; IHC, inner hair cell; LER, lesser epithelial ridge; Mo, morphologic examination; m, modiolus; MT, middle turn; NF, neural fibres; NTD, neural tube defect; OC, organ of Corti; OHC, outer hair cells; osl, osseous spiral laminae; PBS, paraformaldehyde in sodium phosphate buffer; S, sensory epithelium; SG, spiral ganglion; SGC, spiral ganglion cells; SRμCT, synchrotron radiation-based microcomputed tomography; SV, Stria vascularis; TEM, transmission electron microscopy; V, vestibule.

* Corresponding author. Tel.: +43 512 504 81529; fax: +43 512 504 23175.
*E-mail address:* Joachim.Schmutzhard@i-med.ac.at (J. Schmutzhard).

0736-5748/$36.00 © 2009 ISDN. Published by Elsevier Ltd. All rights reserved.
doi:10.1016/j.ijdevneu.2009.07.008

experimental results suggest an involvement of the inner ear in neural tube defects.

Furthermore the hindbrain has been reported to play an essential role in the development of the inner ear. The kreisler (kr-kr) mutant mouse fails to develop rhombomeres 5 and 6 of the embryologic hindbrain. This neural tube defect is associated with a failure of the development of the endolymphatic duct resulting in a cystic poorly differentiated structure (Ruben, 1973).

In the black eyed white mutant mice (ww$^{v}$6J) a neural crest defect was observed in combination with a lack of intermediate cells in the stria vascularis. These mice became severely deaf in early postnatal development and lack neural crest derived melanocytes (Schrott et al., 1988; Schrott and Spoendlin, 1987).

In the Splotch mutant mouse, a further murine animal model, the relationship between the development of hindbrain and inner ear was demonstrated. This animal model presents with a neural tube defect of varying degree combined with an altered melanocyte migration into the stria vascularis (Buckiova and Syka, 2004). This experimental data suggests an involvement of the human inner ear in anencephaly. In 1980 Friedmann et al. suggested that malformations of the cochlea and vestibule can occur in the anencephaly (Friedmann et al., 1980).

To differentiate neuronal cell population in the developing cochlear nerve a set of markers for immunohistochemistry is available. The soma and the axons of the spiral ganglion cells differentially express the neuron specific beta-III-tubulin (Hallworth and Luduena, 2000). Beta-III-tubulin stains developing neurons throughout the central and peripheral nervous system and is expressed by both immature and mature spiral ganglion neurons hence representing a widely used neuronal marker. Peripherin is a further intermediate filament protein expressed in peripheral neuronal structures. In the adult cochlea peripherin has been shown to selectively label the type II ganglion cells in the spiral ganglion although its function remains unclear. Furthermore an up regulation of peripherin in the ganglion cells has been found after axotomy indicating regeneration and axonal extension (Lallemend et al., 2007; Liu et al., 2008).

Cells from mesenchymal origin are stained with immunohistochemical labeling for vimentin. Cells of epithelial origin are supposed to be void of any immunoreactivity. Therefore, staining for this intermediate filament can detect a regular development and migration of intermediate and basal cells of the stria vascularis (Schrott et al., 1988).

The focus of this study is set on morphological alterations of the cochlea and an immunohistochemical examination of the neuronal and neural crest derived cells. The temporal bones have been investigated morphologically with light- and transmission electron microscopy and synchrotron radiation-based microcomputed tomography (SRμCT) and immunostained with the above mentioned markers to trace migrating neuronal and non-neuronal cells during different developmental stages in inner ears of anencephalic fetuses.

## 1. Experimental procedure

The study was approved by the internal review board of the Innsbruck Medical University. The temporal bones were obtained during routine autopsy at the Institute of Pathology after legal interruptions of pregnancy.

### 1.1. Study design

Temporal bones from 12th to 40th weeks of gestation were included in this study.

Six cases of anencephalus with a total of eight temporal bones and three normally developed control cases were investigated. Two further temporal bones of normally hearing healthy adults were included in this study as a control for immunohistochemical staining patterns. The malformation's characteristics are presented in Table 1. In order to reduce autolysis autopsies were performed 1–5 h after death.

The anencephalic temporal bones were graded into mild, moderate and strong depending on the severity of the pathologic malformation.

Anencephaly/exencephaly was defined as mild defect concording to the following parameters: cranial bones are present, but the cranial roof is missing. Herniation of a sac containing severely damaged brain tissues. The defect is covered by normal scalp (Keeling, 1987).

Anencephaly was counted as moderate malformation with the following definition: absence of the cranial vault, no parietal bones, only small, supraorbital ridges representing the frontal bones, missing squamous occipital bone. Small base of skull, usually no pituitary gland, nor N. optici. No cerebral cortex is detectable; the base of the skull is covered by a cerebrovascular mass consisting of vessels, degenerated brain tissue and ependyma. Sometimes the defect is covered by a membrane or skin (Keeling, 1987).

Craniorachischisis was counted as strong malformation defined on the following parameters: in its minimal form representing anencephaly with absence of the foramen magnum, at the worst comprising craniorachischisis totalis, where the whole length of the neural tube is open (Keeling, 1987).

Three of these temporal bones were used for immunohistochemical investigations on paraffin sections. Prior to sectioning one of the paraffin blocks was used for analysing the gross morphology in a synchotron radiation-based microcomputed tomograph.

The remaining five temporal bones were post-fixed in Karnovsky's fixative for morphological analyses. One was further evaluated with transmission electron microscopy (TEM).

### 1.2. Tissue preparation

After removal temporal bones were immediately fixed by immersion in cold 4% paraformaldehyde in sodium phosphate buffer (PBS), pH 7.2, for 1 week.

Following fixation temporal bones were rinsed several times in ice cold PBS, followed by decalcification with 10% EDTA (Titriplex III® Merk, Darmstadt, Germany) in PBS (pH 7.4) at 37 °C for 3–6 weeks depending on the gestational age. After dehydration in graded ethanol's and embedding in paraffin, blocks were cut in serial 5 μm radial sections. Every ninth and tenth sections was stained both with cresyl violet or hematoxylin–eosin.

For TEM preparation and ultra-structural analysis the specimen was osmified, dehydrated in graded ethanol's, embedded in Spurr's low viscosity resin and

**Table 1**
Specimen overview and clinical evaluation of NTD's and control.

| Specimen | Gender | Age | Examination | Grade | Diagnosis |
|---|---|---|---|---|---|
| 1 | f | 12th g | Mo, T | Strong | Anencephaly, minimal rachischisis |
| 2 | m | 17th g | Mo, I | Moderate | Anencephaly, hypoplasia right face |
| 3a | m | 18th g | Mo | Mild | Secondary anencephaly |
| 3b | m | 18th g | Mo, I, C | Mild | Secondary anencephaly |
| 4 | f | 18th g | Mo | Mild | Anencephaly/exencephaly |
| 5a | f | 20th g | Mo, I | Moderate | Anencephaly |
| 5b | f | 20th g | Mo | Moderate | Anencephaly |
| 6 | m | 40th g | Mo | Moderate | Anencephaly with dystrophy |
| A | m | 16th g | Mo, I | No | Spontaneous abortion, no malformation |
| B | w | 20th g | Mo, I | No | Spontaneous abortion, no malformation |
| C | m | 21st g | Mo, I | No | Spontaneous abortion, no malformation |
| D | m | Adult | Mo, I | No | Cardiac arrest |
| E | f | Adult | Mo, I | No | Cardiac arrest |

NTD: neural tube defect, g: gestational age, Mo: morphologic examination, T: transmission electron microscopy, I: immunohistochemistry, and C: synchotron radiation-based microcomputed tomography.

polymerized for 48 h at 60 °C. 1 μm thick semithin sections were stained with toluidine blue for light microscopic evaluation. 90 nm thick ultrathin sections were cut with a Leica UC6 microtome and transferred to pioloform F (polyvinylacetate) coated (1.5% pioloform in chloroform) slot grids. Staining was performed using an automated system (Leica EM Stain) with uranyl acetate (5 g/l; 30 min) and lead citrate (5 g/l, 50 min) at 25 °C.

### 1.3. Antisera

For Vimentin a monoclonal mouse antibody (Ventana-Roche 790-2917) was applied, anti-beta-III-tubulin (MAB5544), a mouse monoclonal antibody was obtained from Chemicon, Temecula, USA. The antibody is highly reactive to neuronal beta-III-tubulin and does not react with beta-tubulin found in glial cells.

Peripherin was labeled with a rabbit polyclonal antibody (Chemicon, Temecula, USA) that stains a ~57 kDa band cleanly and specifically and shows no cross-reactivity with vimentin or any of neurofilament subunits.

### 1.4. Immunocytochemistry with paraffin-embedded sections for transmitted light microscope

Immunocytochemistry was performed on paraffinized sections with a Ventana® Roche® Discovery Immunostainer according to the DAB-MAP discovery research standard procedure. Briefly, sections were incubated with an antibody against vimentin (ready-to-use), peripherin (1:2000) and beta-III-tubulin (1:500) for 1 h at room temperature. Sections were processed with biotinylated Ventana universal secondary antibody (Ventana 7604205). The detection was achieved using the DAB-MAP Detection Kit (Ventana 760500) according to the diaminobenzidine development method with copper enhancement and lightly counterstained with hematoxylin (Ventana 790-2208). Sections were then manually dehydrated, cleared in xylene and coverslipped. The structural and immunohistochemical results were compared to age matched controls and adult temporal bones.

### 1.5. Synchrotron radiation-based microcomputed tomography

The specimen was prepared and embedded in paraffin as described above.

The SRμCT data were acquired in absorption contrast mode at the beamline BW 2 (HASYLAB at DESY, Hamburg, Germany) using the tomography apparatus operated by the GKSS-Research Center, Geesthacht, Germany (Beckmann, 2002). The photon energy of 10.0 keV was chosen. 721 projections between 0° and 180° were recorded with the optical magnification of 1.92, that leads to a pixel size of 4.68 μm × 4.68 μm. The spatial resolution, experimentally characterized measuring the modulation transfer function (Müller et al., 2001) corresponds to 8.32 μm. Since the monochromatic X-ray beam was almost perfectly parallel, the tomograms were reconstructed slice-wise based on the filtered back-projection algorithm (Kak and Slaney, 1988).

### 1.6. Image processing of the SrμCT data

The software VG Studio Max 1.2.1 (Volume Graphics, Heidelberg, Germany) served for the segmentation and 3D visualization of the anatomical details of the embedded cochlea. The length of the cochlea was measured by means of a software tool that allows marking the trajectory by manual selection of points along the central line of the organ of Corti. The tool is based on the software IDL 7.0 (ITT Visual Information Solutions, Boulder, CO, USA). The results were incorporated into the VG Studio visualization software.

### 1.7. Data analysis

Digital images of immunostained slices were acquired in Image-Pro 6.0 (Media Cybernetics) linked to a 3-CCD color video camera (Sony DXC-950P) and an Olympus BX50 light microscope. Two sections of each specimen were examined by two individuals in a double blinded way. The examiners were instructed to analyse the temporal bone along the entire cochlea.

The evaluation was done in a semi-quantitative manner. Individual staining intensities were arbitrarily graded as not detectable (0), no immunoreactivity (−) and immunoreactivity (+). Special focus was set to the organ of Corti, the stria vascularis, spiral ganglion and the scarpa ganglion neurons.

## 2. Results

The diagnosis of a NTD was confirmed by the Institute of Pathology and the temporal bones were allocated to the grades of severity of the manifestation of the neural tube defect by the pathologist, the latter being graded as mild, moderate or strong (Table 1). Eight NTD temporal bones were included into the study. As a control group three fetal temporal bones and two adult temporal bones from normal hearing individuals were added. The results are summarized in Table 1.

**Table 2**
Morphologic results of NTD's.

| Specimen | SGC | OC | Cochlear turns |
|---|---|---|---|
| 1 | + | + | 2.5 |
| 2 | + | + | 1 |
| 3a | + | + | 2.5 |
| 3b | + | + | 2.5 |
| 4 | + | + | 2.5 |
| 5a | + | + | 2.5 |
| 5b | + | + | 2.5 |
| 6 | + | + | 1 |

NTD: neural tube defect, SGC: spiral ganglion cells, OC: organ of Corti, +: present, and −: not present.

### 2.1. Morphologic examination

All eight neural tube defect and five control temporal bones were evaluated by light microscopy. Temporal bone number 1 was examined with TEM. Temporal bone number 3b was scanned with SRμCT (Table 1).

#### 2.1.1. Light microscopy

Inner ear sections were examined for tissue anatomy of the developing cochlea with special focus to the spiral ganglion, the organ of Corti, the stria vascularis. Six of the eight included Temporal bones displayed a fully developed cochlea with 2.5 turns (Table 2 and Fig. 1a–c).

Temporal bone numbers 2 and 6 had a shortened cochlea with only a single turn (Figs. 1d and 2). The fluid spaces in temporal bone 2 were appeared to be separated in a normal manner into scala tympany, scala vestibuli and the cochlear duct. The developing sensory epithelium was present as well as a considerable amount of spiral ganglion cells (not counted) with central and peripheral processes (Fig. 1d).

The single cochlear turn in temporal bone 6 showed an incomplete separation of the fluid spaces along the cochlea duct (Fig. 2a and b). The modiolus was severely hypoplastic with atypic osseous spiral laminae travelling more baso-apically than radially (Fig. 2b–d). These osseous spiral laminae contained myelinated nerve fibres (Fig. 2e) extending their peripheral axon towards the sensory epithelium that was present but not well preserved in this specimen. Spiral ganglion neurons were located in a shortened but well established Rosenthal's canal sending their central axons into a broad inner ear canal containing the cochlear nerve.

The spiral ganglion could be shown in eight of the included temporal bones. Six of the eight cases did have the known morphological configuration of 1.5 turns.

The organ of Corti or Koellikers organ respectively was present in all anencephalic temporal bones and conformed with the developmental stages in unaffected temporal bones of corresponding age.

#### 2.1.2. Synchotron radiation-based microcomputed tomography (SRμCT)

Temporal bone 3b was analysed with SRμCT and displayed the fully developed 2.5 cochlear turns with an intact cochlear duct. The otic capsule was opened at the apex during drilling. The length of the cochlea represents 17.8 mm length. The cochlear nerve with SGNs and nerve fibres showed a distinct contrast in SRμCT that enabled us to follow neuronal tissue in the 3D dataset (Fig. 1b).

The SRμCT images correlated with the corresponding histomorphological sections (Fig. 1a) confirming rich innervation of the sensory epithelium with by bipolar SGNs.

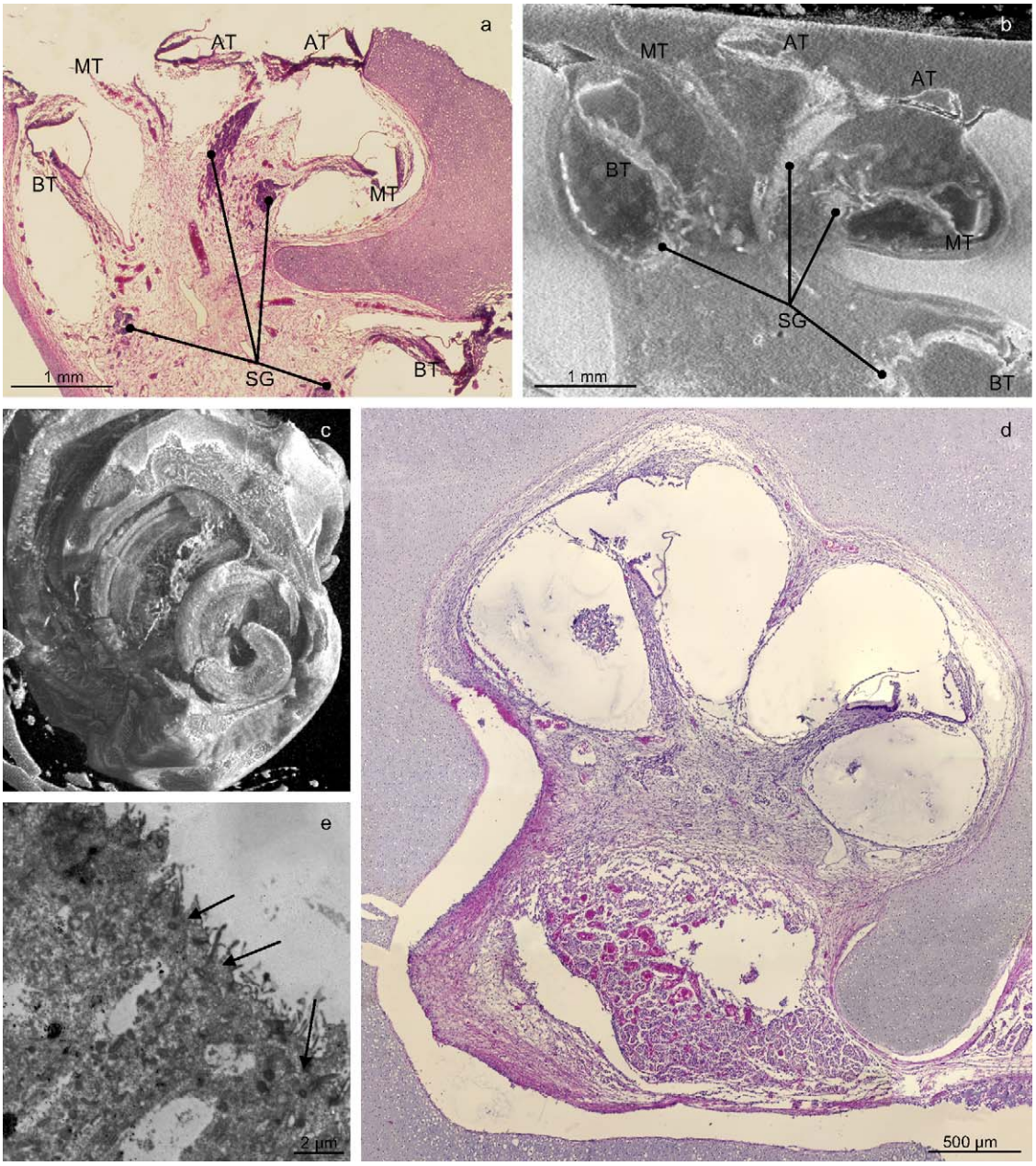


**Fig. 1.** Light microscopy (a and d), SRμCT (b and c) and TEM (e) of anencephalic temporal bones. (a) HE staining of temporal bone 3b (18th g). The otic capsule is opened in the apex, spiral ganglion (SG) and nerve fibres are present—AT, apical turn; BT, basal turn; MT, middle turn. (b) SRμCT image of temporal bone 3b. Corresponding structures identified in (a) are visible—AT, apical turn; BT, the basal turn; MT, the middle turn; SG, spiral ganglion. (c) 3D reconstruction of SRμCT data of temporal bone 3b. Fully developed 2.5 turns were confirmed. (d) HE staining of a midmodiolar section of temporal bone 2 (17th g). The hypoplastic modiolus forms the basic for a shortened cochlea, only a single turn is developed. The nerval structures are regularly developed. (e) Transmission electron microscopic view of the apical surface of supporting cells in the greater epithelial ridge. Basal insertion of kinocilia and the orientation of the accessory centriol (arrows) showed some variable orientation.

### 2.1.3. Transmission electron microscopy

Temporal bone 1 was further examined with transmission electron microscopy. Special interest was set on the exam of the kinocila and the orientation of the basal body. The basal bodies showed various alterations in their orientation (Table 1 and Fig. 1e).

## 2.2. Immunohistochemical examination

Three temporal bones (numbers 2, 3b, 5a) were immunostained for intermediate filaments and vimentin. Staining patterns were compared age related with the control temporal bones A–C and with the adult control temporal bones D and E and findings are summarized in Table 3.

### 2.2.1. Peripherin

Peripherin positive nerve fibres travel within the sensory organ from the habenula via the tunnel of Corti along supporting cells (Deiter cells in more mature stages) towards the outer hair cells indicating strong expression of the intermediate filament in nerve fibres innervating the outer receptor cells (Fig. 3a). In the adult organ of Corti a distinct staining of outer spiral bundles and tunnel spiral bundles is obvious. No reaction was seen in the stria vascularis, the outer and inner hair cells in all temporal bones.

The peripherin staining was seen in all spiral ganglion cells (Table 3) – type I as well as type II – in the temporal bones 2, 3b and 5a (Fig. 3b). A comparable staining pattern was observed in the age

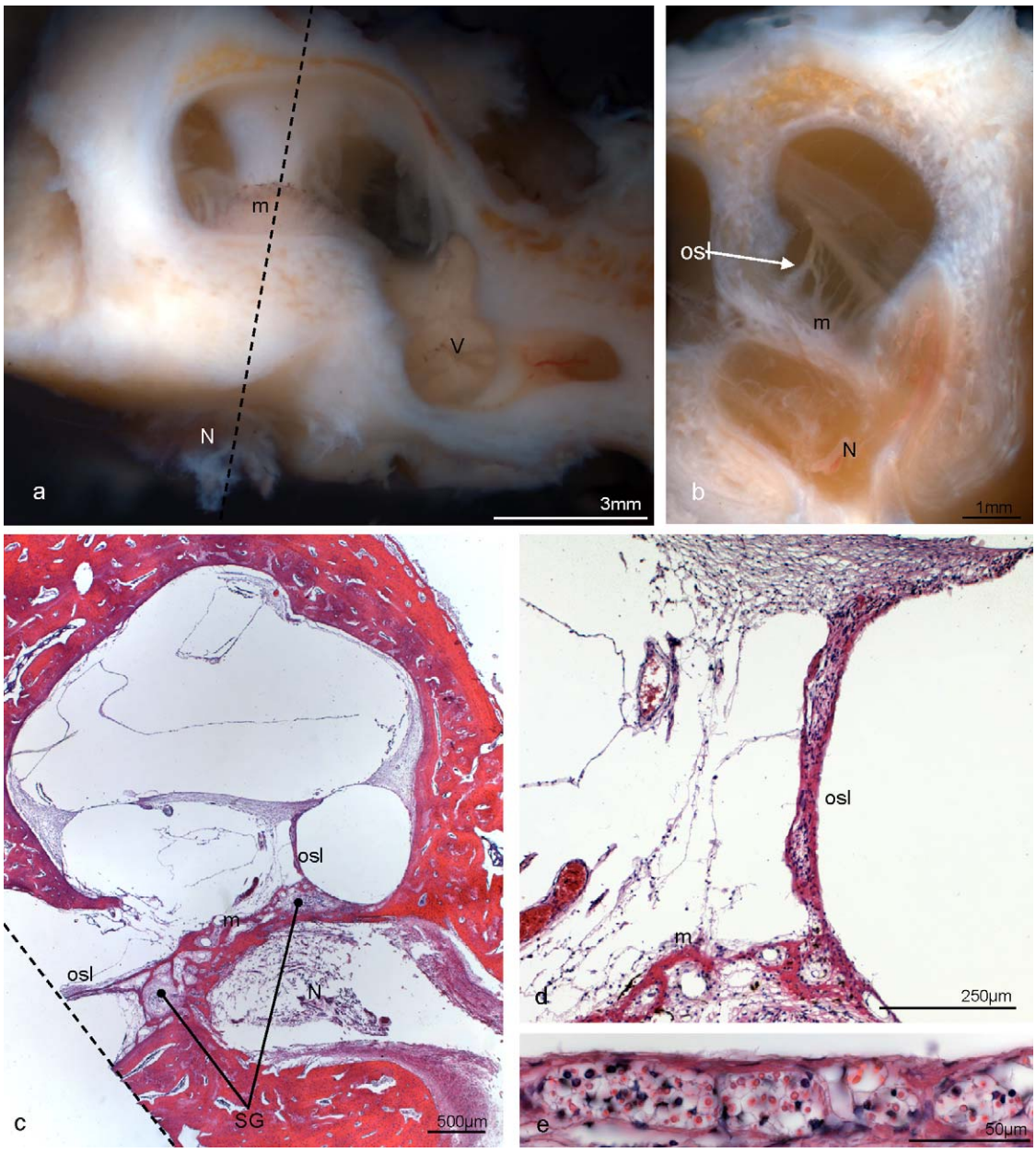


**Fig. 2.** Surface view (a and b) and HE stained sections (c–e) of the anencephalic temporal bone 6 (40th g). (a) Only one turn can be identified with the central modiolar spindle. The dotted line shows the sectioning plane-surface of this sectioning plane visible in (b). V, vestibule. (b) Section through the modiolus as indicated in (a). Osseous spiral laminae (osl) travel baso-apical from the hypoplastic modiolus (m) towards the sensory epithelium. N, cochlear nerve. (c) Section of specimen shown in (b): Rosenthal's canal and the cochlear nerve (N) contain a considerable amount of neural structures. (d) Higher magnified view of (c). The atypic osseous spiral lamina encloses plenty of nerve fibres. m, modiolus. (e) Higher magnification of the osseous spiral lamina in the lower basal turn, a substantial amount of myelinated nerve fibres is visible.

**Table 3**
The immunohistochemical results of NTD's and contol.

| Specimen | Vimentin | | | | Beta-III-tubulin | | | | Peripherin | | | |
|---|---|---|---|---|---|---|---|---|---|---|---|---|
| | SG | OC | SV | NF | SG | OC | SV | NF | SG | OC | SV | NF |
| 2 | + | – | + | + | + | + | – | + | + | – | – | + |
| 3b | + | – | + | + | + | + | – | + | + | – | – | + |
| 5a | + | – | + | + | + | + | – | + | + | – | – | + |
| A | + | – | + | + | + | + | – | + | + | – | – | + |
| B | + | – | + | + | + | + | – | + | + | – | – | + |
| C | + | – | + | + | + | + | – | + | + | – | – | + |
| D | × | × | × | × | × | × | × | × | + | – | – | + |
| E | × | × | × | × | × | × | × | × | + | – | – | + |

NTD: neural tube defects, SG: spiral ganglion, OC: organ of Corti, SV: stria vascularis, NF: neural fibres, +: positive reaction, –: negative reaction, and ×: not included in this study.

matched control temporal bones A–C. In both groups types I and II spiral ganglion cells including their peripheral and central axons were immunopositive, however some neurons showed a more intense staining in their perikaryia (Fig. 3b). In the adult cochlear nerve specific staining for peripherin was present in the small spiral ganglion cells, suggestive for type II neurons.

### 2.2.2. *Beta-III-Tubulin*

Positive staining for beta-III-tubulin was observed in the immature outer and inner hair cells, all spiral ganglion cells and the neuronal fibres (Fig. 3c and d). The staining pattern was equal in the control and the anencephalic group. No staining was detected in the stria vascularis of the control and the neuronal tube defects group (Table 3 and Fig. 3c).

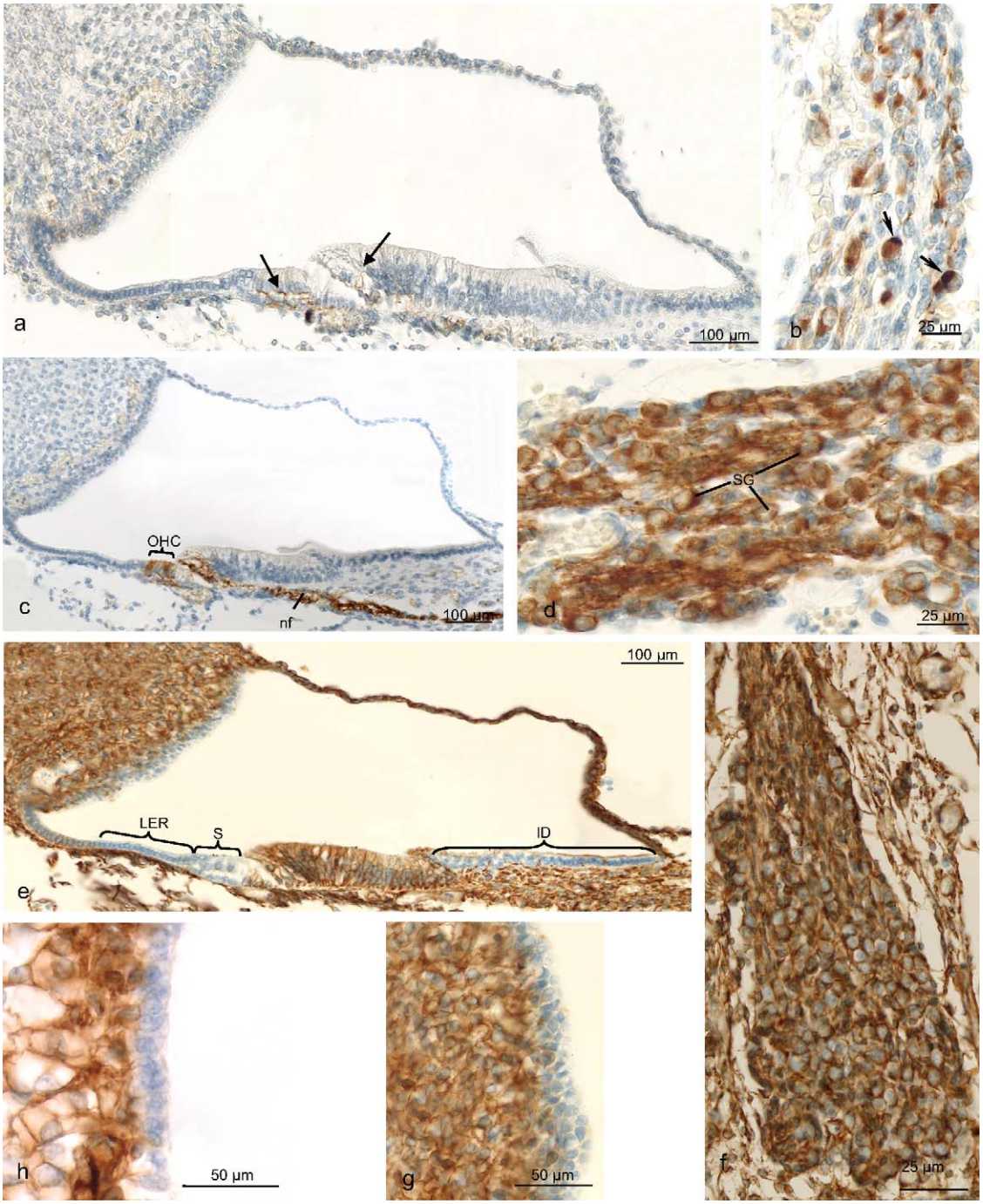


**Fig. 3.** Immunostaining for peripherin, beta-III-tubulin and vimentin staining in the cochlea of an neural tube defect temporal bone and a normal control temporal bones. (a) The cochlea of the anencephalic temporal bone 3b. Nerve fibres beneath the sensory epithelium are labeled for peripherin (arrows). (b) Spiral ganglion neurons show varying intensities of immunoreactivity for peripherin in temporal bone 3b (arrows). (c and d) Immunostaining for beta-III-tubulin of temporal bone 3b: positive staining was recognized in the outer hair cells (OHC), inner hair cells (IHC), the spiral ganglion cells (SG) and the neuronal fibres (nf). (e) Immunostaining for vimentin in temporal bone 3b: the marginal zone of the stria vascularis, the sensory epithelium (S), cells of the lesser epithelial ridge (LER) and interdental cells (ID) were void of any immunoreactivity. (f) Spiral ganglion of temporal bone 3b displaying strong immunostaining for vimentin in the cells surrounding the neurons. (g) Higher magnification of the stria vascularis in (e) confirms absence of immunoreactivity for vimentin in marginal zone. (h) Higher magnified view of the stria vascularis revealed no staining in the marginal zone for vimentin in the control.

*2.2.3. Vimentin*

Vimentin was found to be in cochlear tissue in Schwann cells surrounding the spiral ganglion neurons, intermediate and basal cells of the stria vascularis, nerve fibres, cells of the greater epithelial ridge, outer sulcus cells and the connective tissue in the neural tube defect group as well as the control group (Fig. 3e–h). No staining was detected all temporal bones in the marginal zone of the stria vascularis, the sensory epithelium including inner and outer hair cells, supporting cells as far as the outer sulcus (Fig. 3e–h). The equal staining pattern was detected in the control temporal bones (Table 3).

## 3. Discussion

The relationship of neural tube defects and the inner ear has been examined with a plethora of different animal models showing

various degrees of involvement of the vestibulocochlear system in neural tube defects (Buckiova and Syka, 2004; Curtin et al., 2003; Doudney and Stanier, 2005). Till today only few studies analysed the involvement of the human cochleo-vestibular system in neural tube defects (Friedmann et al., 1980). In 1980 Friedmann et al. described in three individuals with severe neural tube defects the following alterations: the cochlea showed a Mondini type malformation with a poorly developed modiolus that was only present in the basal turn and opened into a wide open bulbous pear-shaped space replacing the upper turns and forming a scala communis. The organ of Corti was well developed, whereas the spiral ganglion cells were diminished considerably (Friedmann et al., 1980).

Our findings partially match this phenotype in two temporal bones. Two of the eight temporal bones (2 and 6) had a shortened cochlea with only a single turn. The hypoplastic modiolus with shortened cochlea is typical for a Mondini inner ear malformation. It was found in temporal bones of different age of development—17th and 40th weeks of gestation. The Mondini type dysplasia is widely present in various congenital disorders such as Turner syndrome (Fish et al., 2009), Pendred syndrome (Yang et al., 2005), Trisomy 13 (Tomoda et al., 1983), Trisomy 22 (Ohtani et al., 2001) or CHARGE syndrome (Wright et al., 1986). An arrest of embryogenesis in the 7th week is supposed to result in 1–1.5 turns or the Mondini type dysplasia (Jackler et al., 1987). Thus the number and preservation of neural perikarya were considerable in these specimens. However, Mondini dysplasia is not very specific to NTDs.

A similar malformation as described in temporal bones 2 and 6 has been described by Padmanabhan (1987) in an murine model, in which exencephaly has been induced with cadmium chloride. A direct toxic effect of cadmium on the vestibulocochlear system has been shown (Ozcaglar et al., 2001). Knowing the toxic effect of cadmium on the adult inner ear, a toxic effect on the developing inner ear is quite likely as already discussed by the author (Padmanabhan, 1987). From our point of view the described inner ear alterations in Padmanabhan's work could be linked to the direct toxic effect of cadmium with a random association with the exencephaly.

The temporal bones with a pathologic alteration only showed a mild or moderate manifestation of the neural tube defect. In our study, we could not correlate the pathologic changes of the cochlear system with the severity of anencephaly. Therefore an expected correlation of the severity of the cochlear malformation and the severity of the grade of anencephaly was not possible in our study. Our data confirms a case series by Smith et al. who described Mondini type deformities of the cochlea in patients with an occipital meningocele. The degree of pathologic changes turned out to be a moderate, survivable version of neural tube defects (Smith et al., 2001). These results can be interpreted by the multifactorial genesis of neural tube defects. A possible way of explanation is the hypothesis that some of the causal mechanisms disturbing neurulation are leading to neural tube defects of different manifestations and additionally to otologic malformations (Doudney and Stanier, 2005; Padmanabhan, 2006).

Epithelial cell polarity genes have been discussed to be involved in NTDs (Doudney and Stanier, 2005). Several murine animal models, such as the Vangl- or the Celsr1 mutation showed planar cell polarity defects that correlated with the development of NTDs (Curtin et al., 2003; Torban et al., 2008) and also affect the inner ear. Curtin described a misorientation of the outer hair cells in the Celsr1 mutation as a result of a disturbed planar cell polarity. Interestingly the gross morphology of the cochlea and the functional testing with Preyer reflex – response to 20 kHz with 90 dB SPL – remained unaltered (Curtin et al., 2003). Similar results were described by Torban et al. who characterized Vangl 1 and 2 mutation. Additionally to the misorientation of the hair cells, a significant reduction of the cochlea size was observed in combination with a craniorachischisis (Torban et al., 2008). The reduction of the cochlea size was not further discussed, limiting the comparability of the here described malformations and murine results.

When screening the various planar cell polarity publications including inner ear studies, barely any gross morphological alterations, like Mondini type malformations, are described (Curtin et al., 2003; Torban et al., 2008; Wang et al., 2006). Comparing the described alterations in the planar cell polarity models with our results, temporal bone 1 has the closest similarities. We found an unchanged gross morphologic cochlea with a severe neural tube defect. Furthermore temporal bone 1 was analysed with TEM, showing various alterations of the orientation of the basal bodies in relation to the referring kinocilia. Assuming that planar cell polarity leads to a misorienation of the stereociliary bundles in the hair cells, the observed misorientation of the basal bodies in temporal bone 1 could be interpreted as a sign of a planar cell polarity disorder (Curtin et al., 2003). Further studies of the cochlea using surface electron microscopy would help to clarify this interpretation.

The intermediate filament beta-III-tubulin is one of the earliest neuronal cytoskeletal marker proteins during development and an established neuronal marker in developmental studies (Katsetos et al., 2003). No difference in the staining pattern was detected comparing the two study groups. Interestingly inner and outer hair cells were immunopositive reflecting the immature stage of sensory cells. It has been previously demonstrated that class beta-III-tubulin is expressed in developing and regenerating sensory hair cells of chicken inner ear (Molea et al., 1999; Stone et al., 1996) whereas it restricts to neural cells in adult animals as described in the guinea pig (Hallworth and Luduena, 2000).

Corresponding to Friedmann's observation a reduction of the spiral ganglion cells should be observed in the anencephalic temporal bone (Friedmann et al., 1980). In the immunohistochemical analysis no reduction of the spiral ganglion cells was seen.

Beta-III-tubulin has also been discussed to be regulated by transcription factors necessary for neuronal lineage commitment and early morphological differentiation (Katsetos et al., 2003) With a regular expression of beta-III-tubulin in both study groups, the likelihood of beta-III-tubulin being fundamentally involved in neural tube defects is decreased.

In the adult spiral ganglion peripherin is known to specifically stain the type II ganglion cells conforming with our results in the adult inner ear. During development peripherin is expressed in spiral ganglion cells as in the type I spiral ganglion cells after axotomy (Lallemend et al., 2007; Liu et al., 2008). Hence, an up regulation of peripherin expression may be interpreted as missing input from the more central parts of the auditory system comparable to axotomy. Our findings did not show any deviation from the staining pattern in anencephalic temporal bones compared to normally developing temporal bones, suggesting normal maturation of the spiral ganglion neurons.

Buckinova et al. found in Splotch mutant mice that morphologic alteration of the inner ear are only found in combination with an anterior neurulation defect. The altered homing of neural crest cells into the vestibulocochlear ganglion was causally discussed (Buckiova and Syka, 2004). To study these migration processes we added immunohistochemitry for vimentin to our study. The neural tube defect temporal bones showed staining in all mesenchymal tissues. Marginal cells of the stria vascularis, the endolymphatic surface and the inner and outer hair cells were void of any immunoreactivity. The equal staining pattern was recorded in our control group. The presence of the intermediate cells in the stria

vascularis indicates a regular migration of intermediate cells from the neural crest into the stria vascularis (Schrott and Spoendlin, 1987). These results differ from Buckiova's findings, which suggest a causal context between the neuralisation defect and an inner ear malformation (Buckiova and Syka, 2004). Our findings in human fetal temporal bones show a regular migration of the intermediate cells from the neural crest into the stria vascularis, which suggests normal development.

The results of this study demonstrate in the eight included temporal bones a wide variety of various cochlear malformations. With our study we could not delineate a distinct malformation of the inner ear, which could be linked to anencephaly. Multifactorial genesis of the neurulation defects hampers the elucidation of inner ear pathologies in anencephaly.

## Acknowledgments

We are very grateful to Mrs. Gunde Rieger for the acquisition of the photographs taken during the ultra-structural analysis. The work was supported by the Austrian Science Foundation Grant 15948-B05.

## References

Beckmann, F., 2002. Microtomography using synchrotron radiation as a user experiment at beamlines BW2 and BW5 of HASYLAB at DESY. Proc. SPIE 34–41.
Buckiova, D., Syka, J., 2004. Development of the inner ear in Splotch mutant mice. Neuroreport 13, 2001–2005.
Cabrera, R.M., Hill, D.S., Etheredge, A.J., Finnell, R.H., 2004. Investigations into the etiology of neural tube defects. Birth Defects Res. C: Embryo Today 4, 330–344.
Copp, A.J., Greene, N.D., Murdoch, J.N., 2003. The genetic basis of mammalian neurulation. Nat. Rev. Genet. 10, 784–793.
Curtin, J.A., Quint, E., Tsipouri, V., Arkell, R.M., Cattanach, B., Copp, A.J., Henderson, D.J., Spurr, N., Stanier, P., Fisher, E.M., Nolan, P.M., Steel, K.P., Brown, S.D., Gray, I.C., Murdoch, J.N., 2003. Mutation of Celsr1 disrupts planar polarity of inner ear hair cells and causes severe neural tube defects in the mouse. Curr. Biol. 13, 1129–1133.
Doudney, K., Stanier, P., 2005. Epithelial cell polarity genes are required for neural tube closure. Am. J. Med. Genet. C: Semin. Med. Genet. 1, 42–47.
Fish III, J.H., Schwentner, I., Schmutzhard, J., Abraham, I., Ciorba, A., Martini, A., Sergi, C., Schrott-Fischer, A., Glueckert, R., 2009. Morphology studies of the human fetal cochlea in Turner syndrome. Ear Hear 1, 143–146.
Friedmann, I., Wright, J.L., Phelps, P.D., 1980. Temporal bone studies in anencephaly. J. Laryngol. Otol. 8, 929–944.
Hallworth, R., Luduena, R.F., 2000. Differential expression of beta tubulin isotypes in the adult gerbil cochlea. Hear Res. 1–2, 161–172.
Jackler, R.K., Luxford, W.M., House, W.F., 1987. Congenital malformations of the inner ear: a classification based on embryogenesis. Laryngoscope 97 (3 Pt 2 Suppl 40), 2–14.
Kak, A.C., Slaney, M., 1988. Principles of Computerised Tomographic Imaging. IEEE Press.
Katsetos, C.D., Herman, M.M., Mork, S.J., 2003. Class III beta-tubulin in human development and cancer. Cell Motil. Cytoskel. 2, 77–96.
Keeling, J.W., 1987. Fetal and Neonatal Pathology. Springer-Verlag, Berlin, Heidelberg.
Lallemend, F., Vandenbosch, R., Hadjab, S., Bodson, M., Breuskin, I., Moonen, G., Lefebvre, P.P., Malgrange, B., 2007. New insights into peripherin expression in cochlear neurons. Neuroscience 1, 212–222.
Lary, J.M., Edmonds, L.D., 1996. Prevalence of spina bifida at birth—United States, 1983–1990: a comparison of two surveillance systems. MMWR CDC Surveill. Summ. 2, 15–26.
Liu, W., Bostrom, M., Rask-Andersen, H., 2008. Expression of peripherin in the pig spiral ganglion—aspects of nerve injury and regeneration. Acta Otolaryngol. 1–7.
Molea, D., Stone, J.S., Rubel, E.W., 1999. Class III beta-tubulin expression in sensory and nonsensory regions of the developing avian inner ear. J. Comp. Neurol. 2, 183–198.
Müller, B., Thurner, P., Weitkamp, T., Rau, C., Bernhardt, R., Karamuk, E., Eckert, L., Buchloh, S., Wintermantel, E., Scharnweber, D., Worch, H., 2001. Non-destructive three-dimensional evaluation of biocompatible materials by micotomography using synchotron radiation. Proc. SPIE 178–188.
Murdoch, J.N., Doudney, K., Paternotte, C., Copp, A.J., Stanier, P., 2001a. Severe neural tube defects in the loop-tail mouse result from mutation of Lpp1, a novel gene involved in floor plate specification. Hum. Mol. Genet. 22, 2593–2601.
Murdoch, J.N., Rachel, R.A., Shah, S., Beermann, F., Stanier, P., Mason, C.A., Copp, A.J., 2001b. Circletail, a new mouse mutant with severe neural tube defects: chromosomal localization and interaction with the loop-tail mutation. Genomics 1–2, 55–63.
Ohtani, I., Kano, M., Sagawa, Y., Ogawa, H., Suzuki, C., 2001. Temporal bone histopathology in trisomy 22. Int. J. Pediatr. Otorhinolaryngol. 2, 137–141.
Ozcaglar, H.U., Agirdir, B., Dinc, O., Turhan, M., Kilincarslan, S., Oner, G., 2001. Effects of cadmium on the hearing system. Acta Otolaryngol. 3, 393–397.
Padmanabhan, R., 2006. Etiology, pathogenesis and prevention of neural tube defects. Congenit. Anom. (Kyoto) 2, 55–67.
Padmanabhan, R., 1987. Abnormalities of the ear associated with exencephaly in mouse fetuses induced by maternal exposure to cadmium. Teratology 1, 9–18.
Rintoul, N.E., Sutton, L.N., Hubbard, A.M., Cohen, B., Melchionni, J., Pasquariello, P.S., Adzick, N.S., 2002. A new look at myelomeningoceles: functional level, vertebral level, shunting, and the implications for fetal intervention. Pediatrics 3, 409–413.
Ruben, R.J., 1973. Development and cell kinetics of the kreisler (kr-kr) mouse. Laryngoscope 9, 1440–1468.
Schrott, A., Egg, G., Spoendlin, H., 1988. Intermediate filaments in the cochleas of normal and mutant (w/wv, sl/sld) mice. Arch. Otorhinolaryngol. 4, 250–254.
Schrott, A., Spoendlin, H., 1987. Pigment anomaly-associated inner ear deafness. Acta Otolaryngol. 5–6, 451–457.
Smith, O.D., Neumann Jr., A.M., Sirimanna, K.S., 2001. Occipital meningocele and Mondini deformity of the cochlea. J. Laryngol. Otol. 1, 71–73.
Stone, J.S., Leano, S.G., Baker, L.P., Rubel, E.W., 1996. Hair cell differentiation in chick cochlear epithelium after aminoglycoside toxicity: in vivo and in vitro observations. J. Neurosci. 19, 6157–6174.
Tomoda, K., Shea, J.J., Shenefelt, R.E., Wilroy, R.S., 1983. Temporal bone findings in trisomy 13 with cyclopia. Arch. Otolaryngol. 8, 553–558.
Torban, E., Patenaude, A.M., Leclerc, S., Rakowiecki, S., Gauthier, S., Andelfinger, G., Epstein, D.J., Gros, P., 2008. Genetic interaction between members of the Vangl family causes neural tube defects in mice. Proc. Natl. Acad. Sci. U.S.A. 9, 3449–3454.
Wang, Y., Guo, N., Nathans, J., 2006. The role of Frizzled3 and Frizzled6 in neural tube closure and in the planar polarity of inner-ear sensory hair cells. J. Neurosci. 8, 2147–2156.
Welsch, F., 1992. In vitro approaches to the elucidation of mechanisms of chemical teratogenesis. Teratology 1, 3–14.
Wright, C.G., Brown, O.E., Meyerhoff, W.L., Rutledge, J.C., 1986. Auditory and temporal bone abnormalities in CHARGE association. Ann. Otol. Rhinol. Laryngol. 5 (Pt 1), 480–486.
Yang, J.J., Tsai, C.C., Hsu, H.M., Shiao, J.Y., Su, C.C., Li, S.Y., 2005. Hearing loss associated with enlarged vestibular aqueduct and Mondini dysplasia is caused by splice-site mutation in the PDS gene. Hear Res. 1–2, 22–30.